

Blocking of NF-κB/p38 MAPK pathways mitigates oligodendrocyte pathology in a model of neonatal white matter injury

Mohamed A. Al-Griw^{1*}, Michael G. Salter² and Ian C. Wood³

¹ Department of Histology and Genetics, Faculty of Medicine, University of Tripoli, Tripoli, Libya,

² Thornton-le-Moor, North Yorkshire, United Kingdom,

³ Faculty of Biological Sciences, University of Leeds, Leeds, United Kingdom,

* Email: m.algriw@uot.edu.ly

Reactive gliosis and inflammation are risk factors for white matter injury (WMI) development, which are correlated with the development of many neurodevelopmental deficits with no treatment. This study aimed to understand the mechanisms correlated with WMI, with a particular focus on the role of nuclear factor-kappa B (NF-κB) and p38 mitogen-activated protein kinases (MAPKs) pathways. Seven-day-old Wistar rats were used to generate cerebellar tissue slices. Slices were cultured and randomly allocated to one of 3 groups and treated as follows: group-I (control); group-II (WMI), slices were subjected to 20 min of oxygen-glucose deprivation (OGD); group-III (WMI+ blockers), slices were subjected to OGD and treated with the blockers. Results showed that OGD insult triggered a marked increase in the apoptosis among WM elements, as confirmed by TUNEL assay. Immunocytochemical experiments revealed that there was a significant decrease in the percent of MBP⁺ OLs and NG2⁺ OPCs, and myelin integrity. There was also a significant increase in the percent of reactive microglia and astrocytes. BrdU immunostaining revealed there was an increase in the percent of proliferating microglia and astrocytes. Q-RT-PCR results showed OGD upregulated the expression levels of cytokines (TNF-α, IL-1, IL-6, and IL-1β) and inducible nitric oxide synthase (iNOS). On the other hand, treatment with BAY11 or SB203580 significantly enhanced the OL survival, restored myelin loss, and reduced microglia and astrocyte reactivity, and downregulated the iNOS and cytokine expression. Our findings demonstrate that blocking of NF-κB/p38 MAPK pathways alleviated reactive gliosis, inflammation, and OL loss upon WMI. The findings may help to develop therapeutic interventions for WMI.

Key words: white matter, NF-κB, p38 MAPK, reactive gliosis, astrocytes, microglia, inflammation, cytokines, iNOS

INTRODUCTION

Increasing evidence suggest that glial cells, mainly microglia and astrocytes, are actively involved in many central nervous system (CNS) pathological conditions (Nakajima and Kohsaka, 1993; Malta et al., 2019; Hara et al., 2020). Injury to the axons, activated microglia, astrocytosis, apoptosis and necrosis of immature oligodendrocytes (OLs) along with disruption of myelin are hallmark pathological features of white matter injury (WMI) (Matute, 2011; Back, 2017; Fern and Matute, 2019). Neuroinflammation plays critical

roles in a number of pathological conditions (Yi et al., 2014). Inflammatory response following CNS injury is important for cleaning of tissue debris, remodeling, and repair of the tissues (Ghasemlou et al., 2010). However, the persistent post-ischemic inflammatory response could contribute to secondary tissue damage (Deng, 2010). It was reported that OL cytotoxicity is mediated via cytokines and reactive oxygen species (ROS) (Merrill et al., 1993; Sherwin and Fern, 2005). Understanding how reactive gliosis and inflammation contribute to OL pathology with a subsequent loss of appropriate myelination after ischemic WMI is likely

to suggest therapeutic approaches to WM disorders (Yin et al., 2018).

Although it has been widely reported that proinflammatory cytokines and ROS play crucial roles in brain ischemic injury, the interactions between astrocytes, microglia, and OL lineage cells are partially understood (Burda et al., 2016). In this study, the effect of ischemia-induced astrocyte and microglia activation on the integrity of OL lineages and myelin was investigated. Use of pharmacological blockers of p38 mitogen-activated protein kinases (p38 MAPKs) and nuclear factor-kappa B (NF- κ B) signaling pathways helped to define how treatment influences the interplay of reactive gliosis on cytokine and inducible nitric oxide synthase (iNOS) expression, OL population survival and myelin disruption after simulated ischemia. We found that blocking of NF- κ B and p38 MAPK signaling pathways after WMI altered this scenario into one leading to preserved WM architecture. This protection correlated with modulated microglia and astrocyte activation, reduced cytokine and iNOS expression, enhanced OL lineages, and preservation of myelin.

METHODS

Ethics statement

All animal experiments were carried out in accord with the regulations of the Research Ethics Committee of the Faculty of Biological Sciences at the University of Leeds and under the provisions of the UK Animals (Scientific Procedures) Act 1986.

Ex vivo cerebellar slice system

Methods were based on previously published protocols (Stoppini, 1991; Al-Griw et al., 2021). Briefly, brains from Wistar rats (postnatal day 7; P7) were used to generate cerebellar tissue slices, where the white matter (WM) is developing and maintain that are equivalent in maturation stage to the human fetus. Pups were sacrificed, and the cerebellar were dissected and transversely sliced at a thickness of 300 μ m on a vibratome (Leica, Germany). Eight to ten tissue slices from 4 to 6 littermates were carefully transferred onto humidified 1.0 μ m pore size cell culture inserts (Millipore, Falcon, UK) and placed in a 6-well plate (Falcon). Cultures were maintained in 1 ml of serum-based medium (50% minimum essential medium Eagle (MEME, Sigma), 25% HBSS (hanks balanced salt solution, Invitrogen), 20% normal horse serum (Invitrogen), 4.6 mM, (v/v) L-glutamine (Sigma), 21 mM (v/v) D-glucose (Fisher Scien-

tific, UK), 1% penicillin/streptomycin solution (Invitrogen), 4.2 μ M (v/v) L-ascorbic acid (Aldrich-Sigma) and 11 mM (v/v) NaHCO₃ at pH 7.2–7.4) in a humidified aerobic incubator (5% CO₂) at 37°C for 3 days. Thereafter, cultures were transferred to serum-free medium supplemented with 0.3 % B27 growth supplement (Invitrogen) and kept for up to 40 days at 37°C in 5% CO₂ with media changes performed twice a week.

Induction of white matter injury

WMI was simulated by exposing 7-day-old cultures to 20 min oxygen-glucose deprivation (OGD) insult. Briefly, the tissue slices were transferred into filter-sterilized, deoxygenated glucose-free culture medium for 20 min in an anaerobic airtight chamber with a mixture of 95% N₂ / 5% CO₂ gas flow, temperature maintained at 37 \pm 0.5°C. After OGD-insult, the cultures were washed at least three times with fresh oxygenated culture medium containing 5 mg/ml D-glucose and supplemented with 3% B27 and returned to their culture conditions under normoxic atmosphere (5% CO₂) at 37°C. Non-OGD treated cultures (control cultures) were maintained for the same time under normoxic conditions. The non- or treated-OGD cultures were further incubated for 3 days as reperfusion period before being fixed for analysis.

Experimental group design

The tissue culture slices were randomly allocated to one of 3 groups and treated as follows: group-I (control), the tissue slices were cultured under normoxic conditions at 37 \pm 0.5°C at the time-points corresponding to that in other experimental groups; group-II (WMI), the tissue slices were cultured and subjected to 20 min of OGD insult in an atmospheric perfusion airtight chamber (95% N₂/ 5% CO₂) gas flow at 37 \pm 0.5°C. Group-III (WMI+ blockers), cultured tissue slices were subjected to 20 min of OGD insult and then were treated with the blockers or vehicle alone (0.1% (DMSO) dimethyl sulfoxide). All test pharmacological agents were added to culture medium 20 min after the OGD end and maintained in the culture medium for 60 min. Appropriate controls were performed at the corresponding time-points with these blockers to test their cytotoxicity.

Drug administration

An NF- κ B blocker BAY11-7082 (Calbiochem, Gibbstown) was dissolved in DMSO as 10 mM stock. A selec-

tive iNOS blocker 1400W dihydrochloride (Sigma-Aldrich) was dissolved in DMSO as 10 mM stock. A p38 MAPK blocker SB203580 (Tocris Cookson) was dissolved in DMSO as 10 mM stock. The blockers were stored in stock solutions at -20°C .

Cell survival assay

Cell survival was measured using a Live/dead Viability/Cytotoxicity kit in accordance with manufacturer's instructions (Molecular Probes, Invitrogen, UK). Briefly, tissue slices were further incubated in the presence of a combined solution containing $4\ \mu\text{M}$ ethidium homodimer-AM (EthD-1) and $2\ \mu\text{M}$ calcein-AM (Cal) at 37°C for 30–45 min, and were then fixed in 4% paraformaldehyde (PFA, Sigma, UK) in phosphate-buffered saline (PBS, Oxoid, UK) for 30 min at room temperature. Using confocal microscopy, viable cells showed the green fluorescence of Cal whilst nuclei of dead cells were indicated by the red fluorescence of EthD-1.

TUNEL assay

Apoptosis was identified at single cell level based on labeling of DNA strand breaks using TUNEL (terminal deoxynucleotidyl transferase-mediated dUTP digoxigenin nick-end labeling OH ends in genomic DNA with fluorescein) detection kit in accordance with manufacturer's recommendation (Chemicon, ApopTag Fluorescein in Situ Apoptosis Detection kit, UK). Briefly, tissue slices prepared and cultured as described above, were then fixed with 4% PFA in PBS for 30 min at room temperature. The fixed slices were incubated in working strength terminal deoxynucleotidyl transferase (TDT) enzyme for 1 h at 37°C in dark, and the reaction was then stopped by stop/wash buffer, and finally fluorescent dye DAPI (4, 6-diamidino-2-phenylindole, Vector Laboratories, UK) was applied to stain nuclei. Non-specific staining was examined by omission of the TDT in the labeling procedure.

Cell proliferation studies

Proliferating cells were detected by using the DNA replication marker 5-bromo-2'-deoxyuridine (BrdU, Sigma-Aldrich, UK), a thymidine analogue that incorporates into the DNA of all cells during the S-phase of the cell cycle (Nowakowski et al., 1989). Cultured tissue slices were incubated in medium containing $20\ \mu\text{M}$ BrdU for 3 or 24 h prior to fixation. The fixed cultures were incubated with 1N HCl for 10 min on ice followed

by 10 min incubation with 2N HCl at room temperature before placing them in an incubator at 37°C for 20 min. To neutralize acid, slices were incubated with borate buffer (0.1 M, pH=8.5) for 12 min at room temperature, followed by three 5 min washing in PBS with 1% Triton 100-X. The slices were subsequently permeabilized in a solution containing PBS (1M) with 1% Triton 100-X, glycine (1 M) and 5% normal goat serum for 1 hr prior to incubation overnight with anti-BrdU mono-antibody (eBioscience, UK) at a dilution 1:50 in PBS followed by DAPI labelling of nuclei.

Immunocytochemistry

For immunocytochemical analysis, the cultured slices were fixed in 4% PFA in PBS for 60 min at room temperature. Following 3 washes with PBS, the slices were mounted on glass and were then blocked for 1 hr at room temperature with a serum blocking solution (10% normal goat serum (MP Biomedical), 0.25% Triton 100-X (Sigma, UK) in PBS. Primary antibodies were diluted in PBS and were then incubated for 24 h at 4°C in the dark. The slices were washed 3 times for 5 min in PBS and secondary antibodies diluted in PBS were added for 2 h at room temperature in the dark, followed by three washes in PBS. The sections were incubated with $100\ \mu\text{l}$ of primary antibody (anti-MBP, MBL; anti-NG2, Millipore; Anti-GFAP; Sigma; and anti-OX-42; Abcam) for 90 min at room temperature or overnight in dark at 4°C . The sections were then washed three times for 5 min in PBS, stained with secondary antibodies (Alexa Fluor® 633 and 488) (Invitrogen, Germany), which were diluted in PBS (at 1:100), for 2 h at room temperature in the dark, and then washed three times in PBS. DAPI was used for morphological assessment of nuclei. To examine the specificity of immunolabelling with the antibodies, control tissues were processed without primary antibodies, which resulted in no immunostaining.

Cell quantification and pixel intensity measurement

Immunopositive cells were counted in 5 randomly selected fields per slice with 3 slices per animal per condition with at least 4 independent biological replicates under $63\times$ magnifications using 9 predetermined grid sections outlined manually using ImageJ (National Institutes of Health, MA) with a grid size, $400\times 300\ \mu\text{m}$; counting frame, $25\times 25\ \mu\text{m}$; z-depth $50\ \mu\text{m}$.

Quantitative analysis of the immunoreaction intensity (pixel intensity) was performed in a series of confocal immunofluorescence images (z-depth $50\ \mu\text{m}$)

at 40 \times magnification (1024 \times 1024 pixels) using ImageJ as previously described (Olivier et al., 2009).

Assessment of WMI

Imaging of immunostained slices was performed by inverted or upright Zeiss LSM 510 Meta confocal laser scanning microscope with HeNe and argon lasers (Carl Zeiss, Inc., Germany) with confocal configuration 405 nm (DAPI, blue), 488 nm (FITC, green), 543 nm (rhodamine, red), and 633 nm (cy5, red) fluorescence.

OL injury of WM was assessed by counting total number of MBP⁺ OLs and the number of pyknotic (TUNEL⁺) OLs in 3 microscopic fields from cerebellum of each brain slice by a blinded observer to the experimental conditions as described previously (Mangin et al., 2012). Morphological characteristics of pyknotic OLs were also counted. Pyknotic OLs were identified by specific morphologic characteristics: pyknotic nuclei, condensed cytoplasm, and/or fragmented processes (Back et al., 2002). The number of viable OL lineage cells per field was recorded as total cells minus pyknotic cells.

Expression studies

Total RNA was extracted from the cultured cerebellar tissue slices using TRIzol (Invitrogen), and cDNA was synthesized by using Super Script II reverse transcriptase (Invitrogen). Quantitative real-time reverse transcriptase polymerase chain reaction (Q-RT-PCR) was performed with a Rotor Gene 6000 PCR analyzer (Corbett Research, UK) with primers described in Table 1. Specificity of PCR amplification and the absence of primer dimers were confirmed by analysis of cycling and melting curves. To further confirm appropriate amplification, the size of amplicons was verified on gel electrophoresis and sequencing. Transcript levels from each were normalized to U6.

Statistics

Findings were analysed using the GraphPad Prism software version 7.0. All data represent the mean \pm SEM (standard error of the mean) for at least 3 independent experiments performed in triplicate. Normality was assessed using the computerized Kolmogorov-Smirnov test. One way analysis of variance (ANOVA) followed by a *post-hoc* test for multiple comparisons Dunnett's were used to determine statistical significance between the studied groups. *P* values <0.05 were considered statistically significant.

RESULTS

Blockade of NF- κ B/p38 MAPK pathways enhances cell survival upon WMI

Because of activation of NF- κ B and p38 MAPK pathways occurs following brain injury (Kim et al., 2010), we reasoned that treatment either NF- κ B blocker BAY11 or p38 MAPK blocker SB203580 might enhance cell survival upon WMI. To do this, cell survival was measured (Fig. 1A). At 3-days post-WMI, the cell survival was a highly decreased in the WMI group compared to control (P <0.001; Fig. 1A-B), and that treatment with either BAY11 or SB203580 preserved cell survival (Fig. 1B). However, the protection gained by SB203580 was greater than observed with BAY11 (P =0.01, P =0.024, respectively; Fig. 1B). BAY11 and SB203580 had no effects when applied under control conditions (data not shown).

We next asked whether treatment with BAY11- or SB203580-induced protection after WMI involves changes in apoptosis, the TUNEL assay in combination with DAPI-nuclei labelling was carried out (Fig. 1C). At 3-days post-injury, we found that apoptotic (TUNEL⁺) cells were more abundant in the WMI group compared to controls (P <0.001), and that treatment with BAY11 or SB203580 reduced their density (P <0.0012 and P <0.014, respectively; Fig. 1D).

Table 1. Rat mRNA primer sequences used for Q-RT-PCR.

Primer	Reverse primers (5' -3')	Forward primers (5' -3')	Amplicon	Source
U6	aacgcttcacgaatttcgct	ctcgcttcggcagcaca	120 bp	Eurogenetic
IL-1 α	ggaaccagaggaaactg	tgccctctgtccttaaagc	157 bp	Eurogenetic
IL-1 β	tggcagaggacaaaggcttc	ttcccaactggtacatcagc	209 bp	Eurogenetic
IL-6	acagtgaggaatgtcaacaac	cccaactccaatgctctcc	179 bp	Eurogenetic
TNF- α	gggcttgctactcgagttt	tgaacttcggggtgatcg	121 bp	Eurogenetic

Blockade of NF- κ B/p38 MAPK pathways restores OLs upon WMI

We next evaluated the impacts of NF- κ B/p38 MAPK pathways on myelin status after WMI. To this end, we quantitatively measured MBP expression in all experimental groups (Fig. 2A). No MBP loss was seen in controls ($P<0.001$; Fig. 2A-B). At 3 days post-WMI, there was a marked decrease in the MBP expression compared to controls ($P<0.001$; Fig. 2A-B), and that treatment with

either BAY11 or SB203580 protected myelin after WMI (Fig. 2A-B).

Activation of NF- κ B/p38 MAPK pathways was described in OLs in many CNS conditions. We characterized, therefore, the impacts of NF- κ B/p38 MAPK pathways on WMI-induced OL death (Fig. 2C). To this end, we immunostained the tissue sections with antibody to MBP (Fig. 2C). We found that MBP⁺ OLs were more abundant in the WMI group compared to control ($P<0.001$), and that treatment with either BAY11

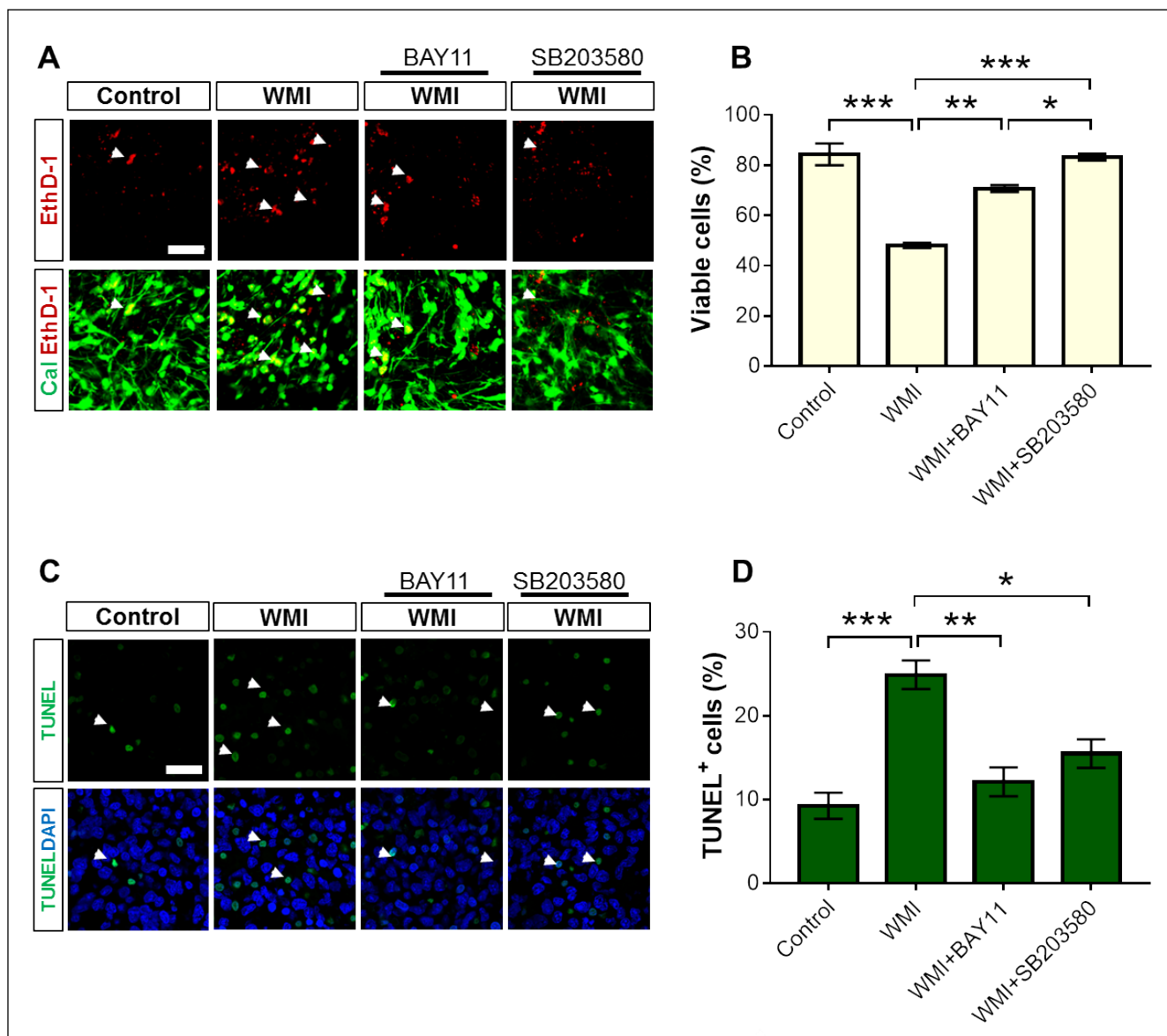


Fig. 1. BAY11 and SB203580 treatment minimizes delayed cell death after WMI. Cerebellar slices were cultured and exposed to conditions of control, WMI, WMI+BAY, or WMI+SB2034580. (A) Representative immunofluorescence images for viable cells (green fluorescence of calcein-AM, Cal) and for dead cells (red fluorescence of ethidium homodimer-AM, EthD-1). Scale bar: 30 μ m. (B) Quantification of cell survival. (C) Representative immunofluorescence images for TUNEL (green) and for DAPI-labelled nuclei (blue). Sale bar: 20 μ m. (D) Quantification of TUNEL⁺ cells. Data are presented as mean \pm SEM. (*) indicates $P<0.05$, (**) indicates $P<0.01$, and (***) indicates $P<0.001$.

or SB203580 restores their density ($P<0.05$, $P<0.049$; Fig. 2D). Together, these findings demonstrate that efficacy of NF- κ B/p38 MAPK blockers in preserving WM architecture.

We next investigated whether the blockade of NF- κ B/p38 MAPK pathways-induced protection for maturing OLs after WMI involves changes in OPC population in this model of WMI. To this end, we immunostained the tissue sections with antibody to NG2, an early OPC marker. We found that NG2⁺ OPCs were more abundant in the WMI group compared to control ($P<0.001$), and that treatment with either BAY11 or SB203580 attenuates their density ($P=0.048$, $P=0.05$; Fig. 3D).

Because of blockade of NF- κ B/p38 MAPK pathways enhanced myelin integrity upon WMI, we postulated that BAY11/SB203580 treatment might affect OPC proliferation. To evaluate OPCs, we double-immunostained the cultured tissue sections for BrdU and NG2 antigen (Fig. 3E-F). We found that BrdU⁺/NG2⁺ cells were more abundant in the WMI group compared to control ($P<0.001$) and that BAY11 or SB203580 treatment enhance the percent of proliferating NG2⁺ OPCs ($P=0.001$, $P=0.005$; Fig. 3F). Moreover, BrdU labelling revealed no statistical difference in the percent of BrdU⁺ OPCs in non- and treated controls with BAY11 or SB203580 (data not shown).

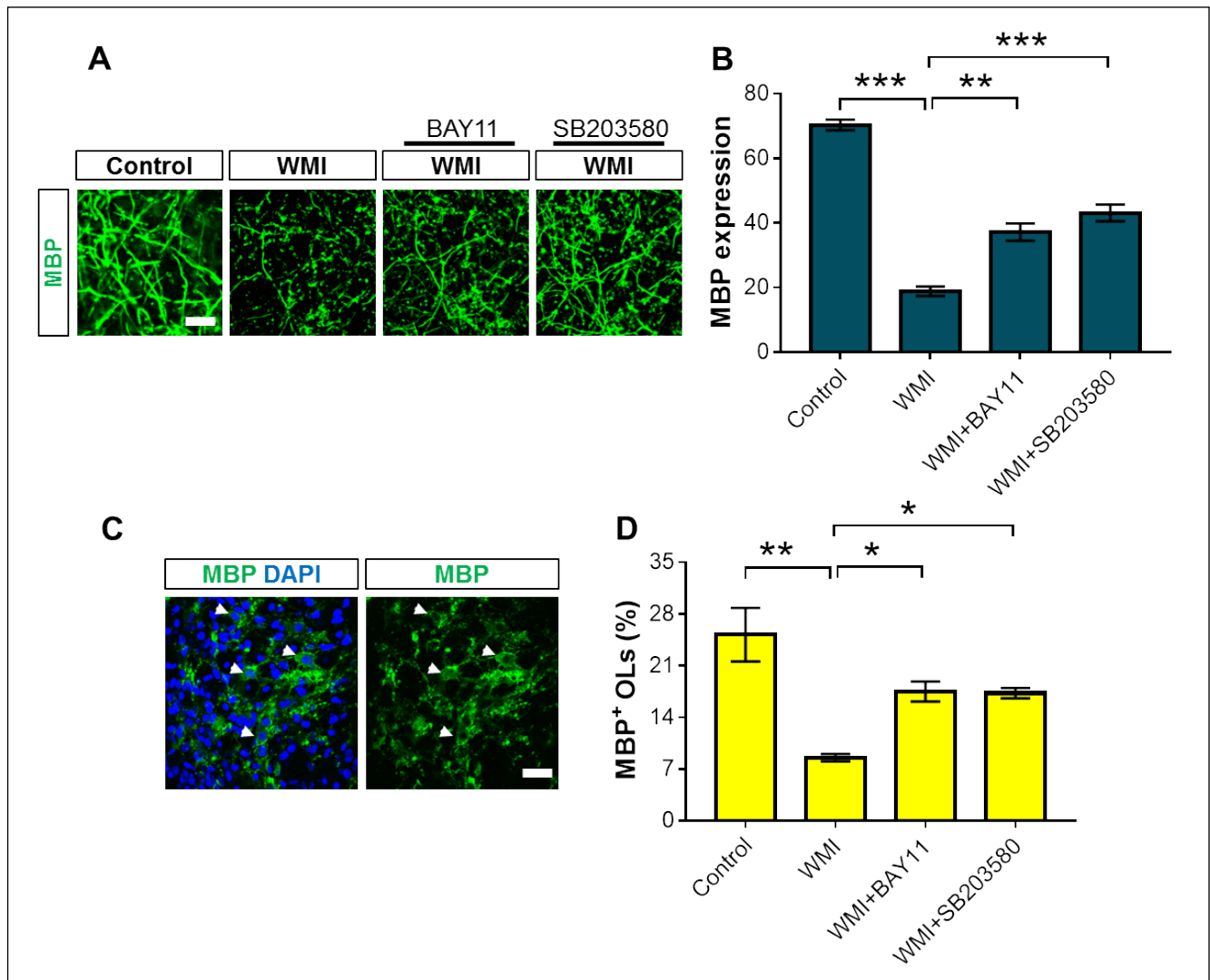


Fig. 2. BAY11 and SB203580 treatment mitigates OLs after WMI. Cerebellar slices were cultured and exposed to conditions of control, WMI+BAY, or WMI+SB2034580. (A) Representative immunofluorescence images of myelin-labeled MBP (green). Scale bar: 20 μ m. (B) Measurement of GFAP expression at 3 days post-injury. (C) Representative immunofluorescence images for MBP⁺ OLs (green) and for DAPI-stained nuclei (blue). (D) Quantification of MBP⁺ OLs at 3 days post-injury. Data are presented as mean \pm SEM. (*) indicates $P<0.05$, (**) indicates $P<0.01$, and (***) indicates $P<0.001$.

Blockade of NF- κ B/p38 MAPK pathways minimizes microglia activation and proinflammatory action upon WMI

As glutamate excitotoxicity might activate microglia and inflammation (Volpe, 2009), we asked whether WMI-mediated inflammation and production of inflammatory mediators, and whether this can be alleviated by blocking of NF- κ B/p38 MAPK pathways. To this end, we quantified OX-42⁺ microglia in immunolabeled the cultured tissue sections (Fig. 4A)

and measured expression of proinflammatory cytokines, including TNF- α , IL-6, IL-1 α , IL-1 β , and iNOS, by Q-RT-PCR (Fig. 4B). We found that OX-42⁺ microglia were more abundant in the WMI group compared to controls ($P < 0.001$; Fig. 4B) and, more importantly, BAY11 or SB203580 treatment reduced the density of activated microglia (OX-42⁺) ($P = 0.02$, $P < 0.0054$; Fig. 4B). Additionally, there was also an upregulation in the TNF- α , IL-6, IL-1 α , and IL-1 β (Fig. 4C), and that treatment with either BAY11 or SB203580 downregulated their levels (Fig. 4C). Consistent with these findings,

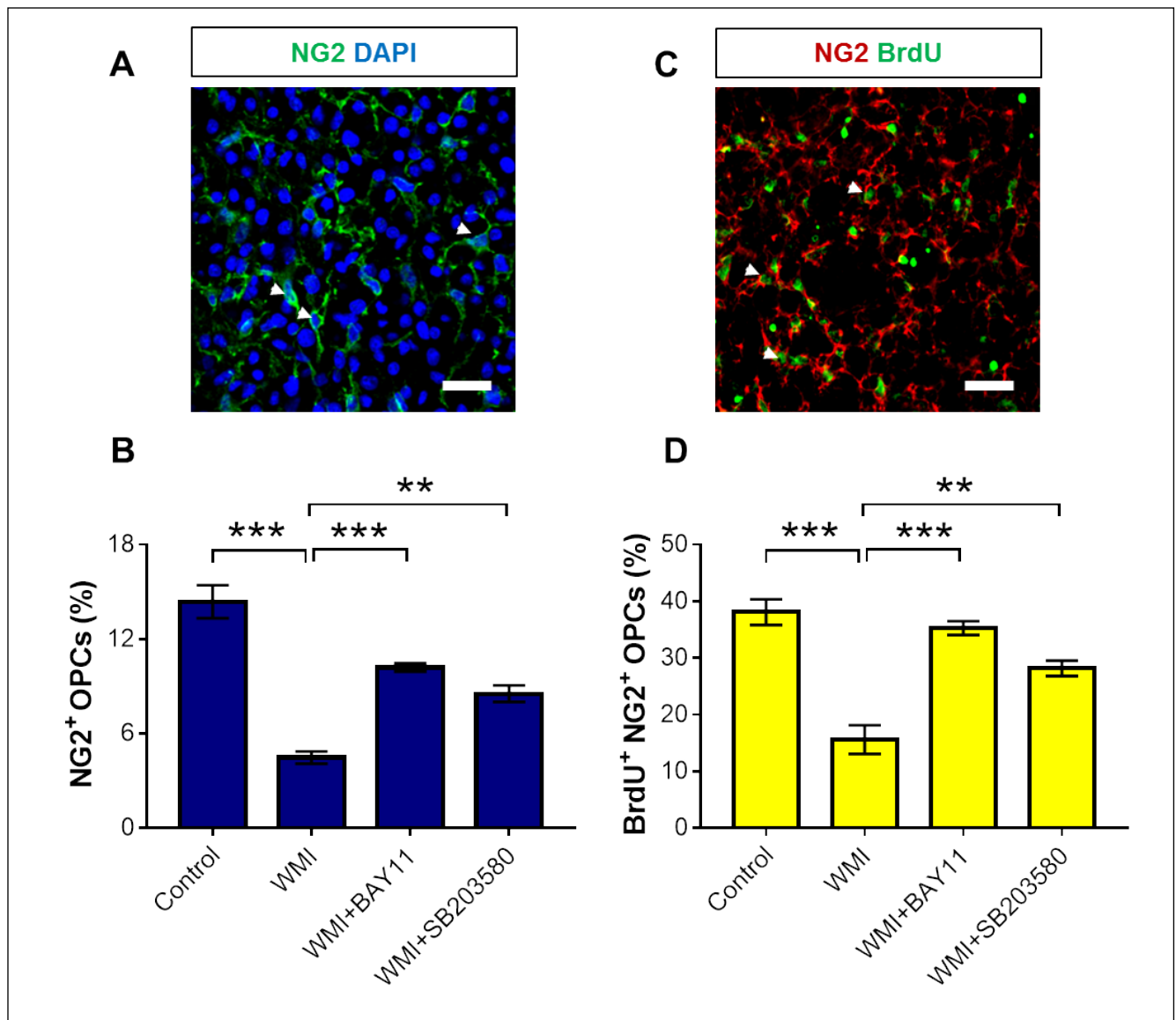


Fig. 3. BAY11 and SB203580 treatment promotes OPC proliferation after WMI. Cerebellar slices were cultured and exposed to conditions of control, WMI, WMI+BAY, or WMI+SB2034580. (A) Representative immunofluorescence images for NG2⁺ OPCs (green) and for DAPI-stained nuclei (blue). Scale bar: 20 μ m. (B) Quantification of NG2⁺ OPCs. (C) Representative immunofluorescence images for BrdU (green) and for NG2 (red). Scale bar: 20 μ m. (D) Quantification of BrdU⁺/NG2⁺ OPCs. (E) Representative immunofluorescence images for BrdU (green) and for NG2 (red). Scale bar: 20 μ m. (F) Quantification of BrdU⁺/NG2⁺ OPCs. Data are presented as mean \pm SEM. (*) indicates $P < 0.05$, (**) indicates $P < 0.01$, and (***) indicates $P < 0.001$.

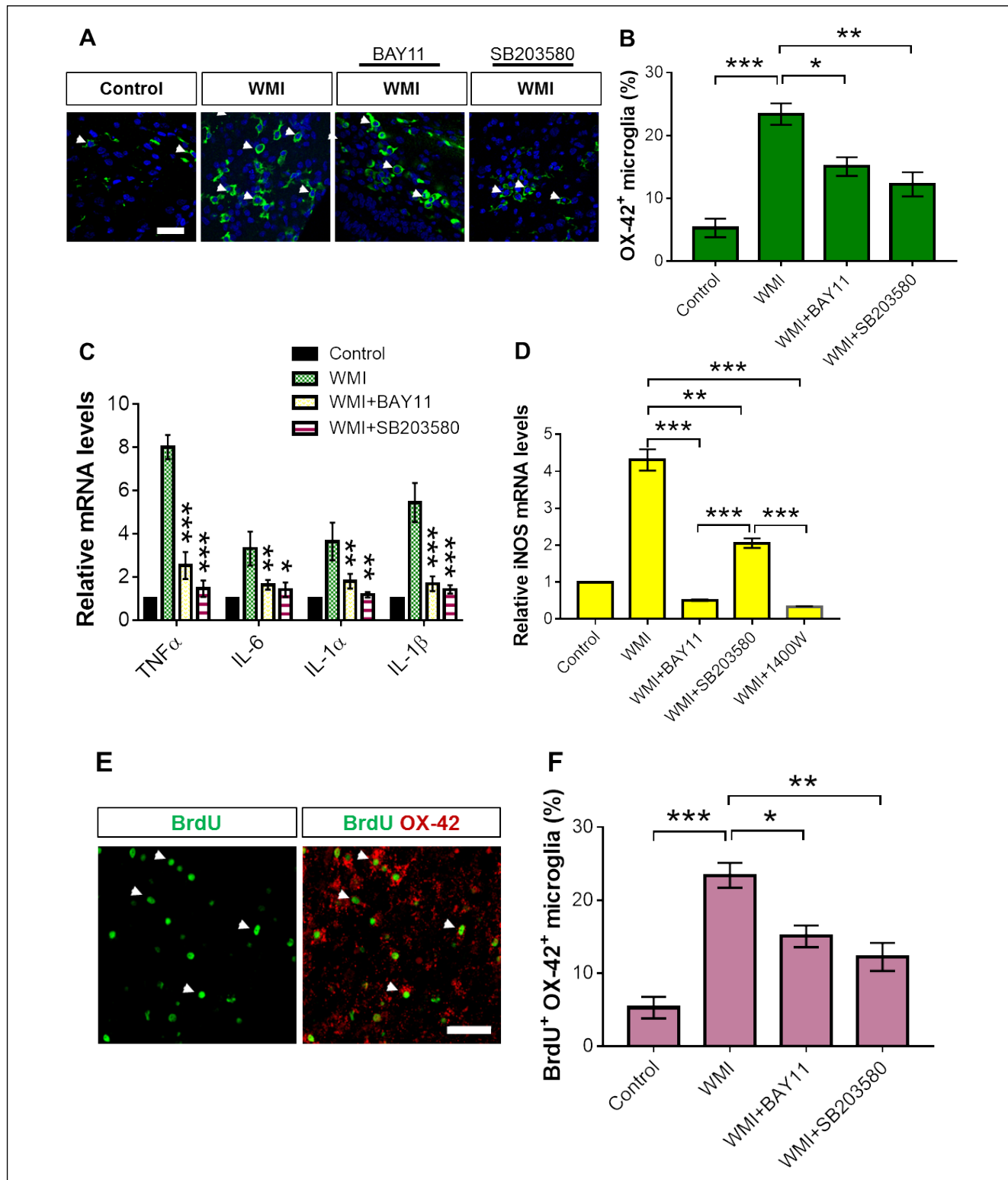


Fig. 4. BAY11 and SB203580 treatment suppresses microglia activation and cytokines after WMI. Cerebellar slices were cultured and exposed to conditions of control, WMI, WMI+BAY, or WMI+SB2034580. (A) Representative immunofluorescence images for OX-42⁺ microglia (green) and for DAPI-stained nuclei (blue). Scale bar: 30 μ m. (B) Quantification of OX-42⁺ microglia. (C) Relative mRNA expression for TNF- α , IL-6, IL-1 α , and IL-1 β at 20 min. (D) Relative mRNA expression for iNOS at 20 min. Data were normalized for the mean of the relative expression of to U6. Expression levels are presented relative to levels in control group, where were set at 1. (E) Representatives co-staining for BrdU (green, arrow) and for OX-42 (red, arrow). Scale bar: 30 μ m. (F) Quantification of BrdU⁺/OX-42⁺ microglia. Data are presented as mean \pm SEM. (*) indicates $P < 0.05$, (**) indicates $P < 0.01$, and (***) indicates $P < 0.001$.

WMI led to an upregulation in the iNOS expression, and that treatment with BAY11, SB203580, or selective iNOS blocker 1400W significantly downregulated its levels (Fig. 4D). However, the protection gained by BAY11 and 1400W was greater than observed with SB203580 ($P=0.0001$; Fig. 4D). BAY11, SB203580, and 1400W had no effects when applied under control conditions (data not shown). This suggests that WMI mediated inflammation is significantly curtailed by BAY11, SB203580, or 1400W treatment.

We next measured the impacts of NF- κ B/ p38 MAPK pathways on the microglia proliferation after WMI. To

this end, the percentage of OX-42⁺ microglia and their colocalization with the mitotic-marker BrdU was measured (Fig. 4E). We found that BrdU⁺/OX-42⁺ cells were highly increased in the WMI group compared to controls ($P<0.001$), and that treatment with BAY11 or SB203580 significantly reduced their density ($P=0.022$, $P=0.002$, respectively; Fig. 4E). Together, these findings indicate that microglia became activated and proliferate in response to ischemia in this model, and that BAY11 and SB203580 treatments resulted in a marked reduction in their activation and proliferation via blocking of NF- κ B/p38 MAPK signaling pathways.

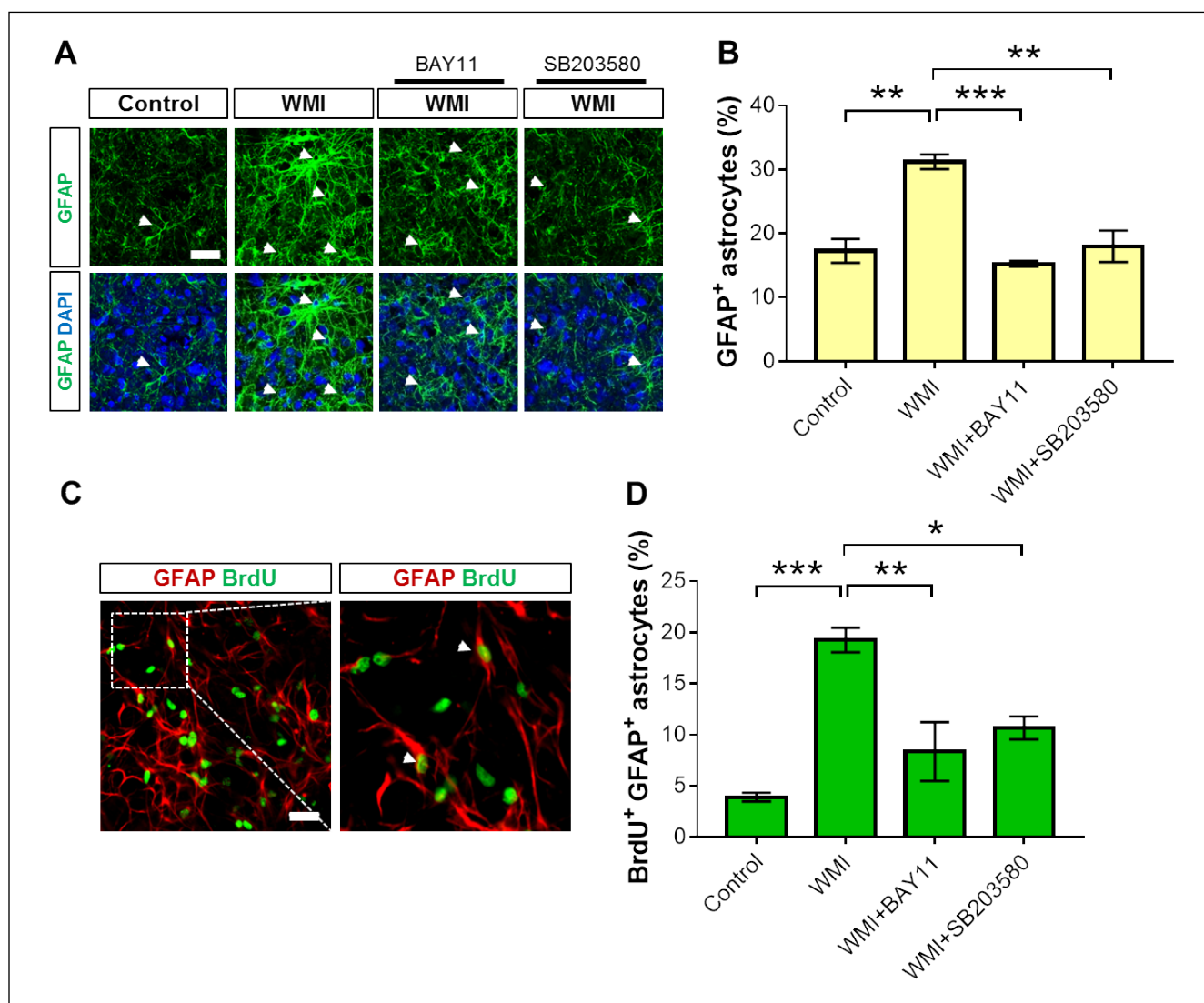


Fig. 5. BAY11 and SB203580 treatment reduces astrogliosis after WMI. Cerebellar slices were cultured and exposed to conditions of control, WMI, WMI+BAY, or WMI+SB2034580. (A) Representative immunofluorescence images for GFAP⁺ cells (green) and for DAPI-stained nuclei (blue). Scale bar: 30 μ m. (B) Measurement of GFAP expression. (C) Representatives immunofluorescence images for BrdU (green) and for GFAP (red) demonstrated that new astrocytes (arrowheads). Scale bar: 30 μ m. (D) Quantification of BrdU⁺/GFAP⁺ astrocytes. Data are presented as mean \pm SEM. (*) indicates $P<0.05$, (**) indicates $P<0.01$, and (***) indicates $P<0.001$.

Blockade of NF- κ B/p38 MAPK pathways reduces astrocyte activation upon WMI

Astrocytes respond to multiple forms of CNS insults such as ischemia and inflammation (Khwaja and Volpe, 2008). GFAP protein upregulation along with astrocyte hyperplasia and hypertrophy are the hallmarks of astrocytosis in response to many CNS pathological conditions (Baltan et al., 2011; Pekny et al., 2014). Here we investigated the impacts of BAY11 and SB203580 treatments on astrogliosis in a model of developing WMI. To this end, we immunostained the cultured tissue sections with antibody to reactive astrocyte-marker glial fibrillary acidic protein (GFAP) (Fig. 5). We found that GFAP expression was significantly increased in the WMI group compared with controls ($P=0.002$; Fig. 5A-B). The increase in the GFAP expression appeared to be due to an increase in the astrocyte process counts and their thickness, commonly seen with reactive astrogliosis (Fig. 5A). However, more importantly, treatment with either BAY11 or SB203580 suppressed astrocyte reactivity ($P=0.02$, $P=0.041$, respectively; Fig. 5B).

We next asked whether the apparent increase in the GFAP expression was caused solely by increased GFAP expression in existing cells or by proliferation of astrocytes. To this end, the percentage of GFAP⁺ astrocytes and their colocalization with the mitotic-marker BrdU was measured (Fig. 5C). We found that BrdU⁺/GFAP⁺ cells were highly increased in the WMI group compared to control ($P<0.001$), and that treatment with either BAY11 and SB203580 reduced the density of reactive astrocytes (GFAP⁺) ($P<0.004$, $P=0.02$, respectively; Fig. 5D).

DISCUSSION

The novel findings in this work were that blocking of the activity of NF- κ B/p38 MAPK signaling pathways after an ischemic episode (OGD insult) mitigated WM pathology and reduced reactive gliosis inflammatory response. Key correlates of these impacts included enhanced MBP⁺ OL and NG2⁺ OPC survival, and reduced myelin disruption, decreased microglia and astrocyte activation and proliferation, and downregulation the expression of cytokines and iNOS. Hence, the current work highlights the role of NF- κ B/p38 MAPK pathways in WMI and suggests a therapeutic opportunity for WMI.

Reactive gliosis is a hallmark of the inflammatory response to multiple forms of CNS insults such as hypoxia-ischemia and inflammation (Khwaja and Volpe, 2008; Deng, 2010; Baltan et al., 2011; Matute, 2011; Pekny et al., 2014; Fern and Matute, 2019). Neuroinflammation plays critical roles in many CNS patho-

logical conditions (Nakajima and Kohsaka, 1993; Yi et al., 2014; Malta et al., 2019; Hara et al., 2020). Following brain injury, inflammatory response is crucial for cleaning of tissue debris and tissue repair (Ghasemlou et al., 2010). However, the persistent post-ischemic inflammatory response could contribute to secondary tissue damage (Deng, 2010). It was found that loss of OL lineage cells is mediated *via* cytokines and ROS (Merrill et al., 1993; Sherwin and Fern, 2005). Understanding how reactive gliosis and inflammation contribute to OL pathology with a subsequent loss of appropriate myelin after ischaemic WMI is likely to suggest therapeutic approaches to WM disorders (Yin et al., 2018).

Injury to the axons, loss of mature and maturing OLs along with disruption of myelin, activated microglia, and astrocytosis are hallmark pathological features of WMI (Matute, 2011; Back, 2017; Fern and Matute, 2019). WMI remains a global health problem and the most common cause of many clinical neurological deficits for which there are no effective treatments (Back, 2017; Fern and Matute, 2019). Recently, we found that WMI triggered a high amount of glutamate release at early and late time periods after the end of OGD insult, and that Na⁺-dependent glutamate transporter-blocker DL-TBOA treatment reduced its release (data not shown). Excess glutamate activates ionotropic glutamate receptors (iGluR) causing iGluR-mediated excitotoxicity, a crucial mediator of the damage WM elements (Follett et al., 2004; Baltan et al., 2011; Butt et al., 2014; Back and Rosenberg, 2014; Fern and Matute, 2019; Robinson et al., 2020). Binding of glutamate to its receptors can promote a further elevation in Ca²⁺ entry (Matute, 2010; 2011; Fern and Matute, 2019). Indeed Ca²⁺ overload upon activation of these receptors can activate multiple putative damaging proteins, such as iNOS, which leads to the ROS.

WMI triggers a cascade of pathological processes. During this event, diverse downstream signaling pathways are recruited, including the NF- κ B and p38 MAPKs (Kim et al., 2010; Saggi et al., 2016; Santa-Cecilia et al., 2016; Wang et al., 2016). p38 MAPK influences the gene expression of cytokines such as TNF- α , IL-1 β , and IL-6, and mediators of oxidative stress (Saklatvala, 2004; Peifer et al., 2006). Expression of cytokines is also modulated by NF- κ B activation (Bianchi et al., 2010). An NF- κ B binding site was identified in the promoter region of the iNOS gene (Xie et al., 1994). In rat forebrain slices exposed to OGD, glutamate was shown to be involved in iNOS expression through the NF- κ B signaling pathway (Cardenas et al., 2000). Increasing evidence suggests that activation of NF- κ B and p38 AMPK pathways occurs following brain injury (Kim et al., 2010; Peixoto et al., 2017). However, there

are conflicting reports on the benefits or detrimental effects of NF- κ B and p38 AMPK in distinct pathological conditions. On the basis of these findings, this work aimed to understand the mechanism(s) correlated with WMI, with a particular focus on the role of NF- κ B/MAPK signaling pathways. Our findings are in general agreement with observations that blocking NF- κ B/p38 MAPK pathways alleviated WM pathology upon ischemic episode.

One key question about WMI is the route by which cell death is triggered, and accordingly, which of signaling pathways could be chosen as a therapeutic target (Shimizu et al., 1999; Andrabi et al., 2019). Using an *ex vivo* slice system of WMI, we found that OGD insult triggered apoptosis as evidenced by TUNEL assay, and that treatment with either NF- κ B blocker BAY11 or p38 MAPK blocker SB203580 reduced their percent. This suggests that apoptosis may be a mechanism by which blockade the activity of NF- κ B/p38 MAPK signaling pathways confers protection against ischemic WMI.

OL lineage cell death and myelin disruption are a central feature of a number of human neurodegenerative disorders, including multiple sclerosis and cerebral palsy (Back and Rosenberg, 2014; Back, 2017; Fern and Matute, 2019; Robinson et al., 2020). There are a number of mutually overlapping mechanisms of OL loss in neurodegenerative disorders. Myelin disruption can occur due to activation of apoptotic cascades induced by cytokines or due to their vulnerability to excitotoxic death. Because of dysregulations of NF- κ B/p38 MAPK pathways was described in many CNS conditions, we characterized, therefore, the impacts of NF- κ B/p38 MAPK pathways on OL lineages and myelin status in the context of WMI. The findings of this study showed that OGD insult damaged OL lineages as shown by the decreased the percent of maturing OLs (MBP⁺) and their precursors (NG2⁺ OPCs) as well as caused myelin disruption, and that blocking of NF- κ B/p38 MAPK pathways strongly preserved OL survival and myelin integrity. The blockade of NF- κ B/p38 MAPK pathways was also effective in preserving NG2⁺ OPC survival and their mitotic behavior. More importantly, this protection was associated with enhanced neural cell survival and reduced apoptosis.

Another major finding in this study is how reactive gliosis-mediated inflammatory response contributes to the deleterious impacts of OGD insult on WM elements in the context of ischemic WMI. Loss of OL lineages is accompanied by diffuse gliosis and disturbances in the composition of the extracellular matrix (Back, 2017; Baltan et al., 2011; Deng, 2010; Fern and Matute, 2019; Khwaja and Volpe, 2008; Matute, 2011; Pekny et al., 2014). Microglia and astrocyte re-

cruitment is also a hallmark of the inflammatory response to hypoxia-ischemia (Deng, 2010; Fern and Matute, 2019). After injury, microglia become activated within minutes to hours, whereas the peak of astrocyte activation occurs within 3 days post-injury (Morin-Richaud et al., 1998). Activation of NF- κ B and p38 MAPK pathways occurs following CNS hypoxia/ischemia (Kim et al., 2010). Because microglia and astrocytes are activated in many CNS insults including ischemic WMI (Matute, 2011), a chance exist for direct impacts of blocking of NF- κ B/p38 MAPK pathways. Using an *ex vivo* slice system of WMI, we found that OGD insult triggered a significant reactive gliosis as shown by the increased the percent of activated and proliferating microglia (OX-42⁺) and astrocytes (GFAP⁺), and that blocking of NF- κ B/p38 MAPK pathways strongly reduced their density. More importantly, this protection was associated with enhanced OL lineage cells and reduced myelin disruption.

Neuroinflammation is a major risk factor for WMI, which is correlated with later development of a number of neurological deficits (Deng, 2010; Fern and Matute, 2019). After injury, microglia triggers a massive inflammatory response further contributed by astrocytes and blood-born macrophages (Deng, 2010; Fern and Matute, 2019). Microglia and astrocyte activation is accompanied by the production of massive proinflammatory mediators including cytokines, ROS, and iNOS (Deng, 2010; Murugan et al., 2011). Production of ROSs triggers inflammation and apoptosis (Dirnagl et al., 1999). Evidence indicates that cytokines (e.g., TNF- α and IL-1 β) (Deng, 2010; Murugan et al., 2011; Peferoen et al., 2014), ROS (Murugan et al., 2011), and iNOS (Yao et al., 2010) are toxic to OL lineages and myelin (Murugan et al., 2011), and interfere with OPC proliferation (Wu et al., 2010). Cytokines such as TNF- α and IL-1 β damages OLs and delayed myelination *via* binding to their respective receptors on the OLs (Deng et al., 2008). OL loss is also thought to result from collateral damage from iNOS in microglia (Yao et al., 2010) *via* NO production (Murugan et al., 2011). ROS, such as NO can react with superoxide anions to form peroxynitrite that can oxidize essential molecules such as DNA, leading to cellular damage (Landi et al., 1994). Upregulated expression of cytokines and its contribution in WM hypoxia was reported (Deng et al., 2009; Sivakumar et al., 2010; Murugan et al., 2011), and was confirmed in this study in the context of ischemic WMI. Specifically, we found that WMI caused an upregulation in the TNF- α , IL-6, IL-1 α , and IL-1 β . We also found that WMI led to an upregulation in the iNOS expression. On the other hand we found that treatment with either NF- κ B blocker BAY11 or p38 MAPK blocker SB203580 downregulated the expression of TNF- α , IL-6, IL-1 α ,

and IL-1 β . In addition, we found that treatment with selective iNOS blocker 1400W significantly downregulated iNOS levels. Taken together, these findings suggest that WMI mediated inflammation is significantly curtailed by BAY11, SB203580, or 1400W treatment. More importantly, this protection was associated with enhanced OL lineage survival, reduced myelin disruption, suppressed microglia and astrocyte reactivity and proliferation.

CONCLUSION

This work highlights the potential role of NF-kB/p38 MAPK pathways in specifically mitigating OL pathology correlated with a number of CNS disorders. In addition, our findings reinforce the linkage between neuroinflammation and myelin disruption. Our findings suggest that reactive gliosis-mediated inflammatory response can develop secondary WM damage that contributes to OL loss, myelin disruption, and development arrest of OPCs through NF-kB/p38 MAPK pathways, a pathway that can be targeting for treatment of WMI.

ACKNOWLEDGEMENTS

The execution of this experiment was supported by the University of Tripoli, Libya.

REFERENCES

- Al-Griw MA, Alghazeer RO, Awayn A, Shamlan G, Eskandrani AA, Alnajeebi AM, Babteen NA, Alansari WS (2021) Selective adenosine A2A receptor inhibitor SCH58261 reduces oligodendrocyte loss upon brain injury in young rats. *Saudi J Biol Sci* 28: 310–316.
- Andrabi SS, Ali M, Tabassum H, Parveen S, Parvez S (2019) Pramipexole prevents ischemic cell death via mitochondrial pathways in ischemic stroke. *Dis Model Mech* 12: dmm033860.
- Back SA (2017) White matter injury in the preterm infant: pathology and mechanisms. *Acta Neuropathol* 134: 331–349.
- Back SA, Han BH, Luo NL, Chricton CA, Xanthoudakis S, Tam J, Arvin, KL, Holtzman DM (2002) Selective vulnerability of late oligodendrocyte progenitors to hypoxia-ischemia. *J Neurosci* 22: 455–463.
- Back SA, Rosenberg PA (2014) Pathophysiology of glia in perinatal white matter injury. *Glia* 62: 1790–1815.
- Baltan S, Murphy SP, Danilov CA, Bachleda A, Morrison RS (2011) Histone deacetylase inhibitors preserve white matter structure and function during ischemia by conserving ATP and reducing excitotoxicity. *J Neurosci* 31: 3990–3999.
- Bianchi R, Giambanco I, Donato R (2010) S100B/RAGE-dependent activation of microglia via NF-kappaB and AP-1 co-regulation of COX-2 expression by S100B, IL-1beta and TNF-alpha. *Neurobiol Aging* 31: 665–677.
- Burda JE, Bernstein AM, Sofroniew MV (2016) Astrocyte roles in traumatic brain injury. *Exp Neurol* 275: 305–315.
- Butt AM, Fern RF, Matute C (2014) Neurotransmitter signaling in white matter. *Glia* 62: 1762–1779.
- Cardenas A, Moro MA, Hurtado O, Leza JC, Lorenzo P, Castrillo A, Bodelon OG, Bosca L, Lizasoain I (2000) Implication of glutamate in the expression of inducible nitric oxide synthase after oxygen and glucose deprivation in rat forebrain slices. *J Neurochem* 74: 2041–2048.
- Deng W (2010) Neurobiology of injury to the developing brain. *Nat Rev Neurol* 6: 328–336.
- Deng Y, Lu J, Sivakumar V, Ling E, Kaur C (2008) Amoeboid microglia in the periventricular white matter induce oligodendrocyte damage through expression of proinflammatory cytokines via MAP kinase signaling pathway in hypoxic neonatal rats. *Brain Pathology* 18: 387–400.
- Deng YY, Lu J, Ling EA, Kaur C (2009) Monocyte chemoattractant protein-1 (MCP-1) produced via NF-kappaB signaling pathway mediates migration of amoeboid microglia in the periventricular white matter in hypoxic neonatal rats. *Glia* 57: 604–621.
- Dirnagl U, Iadecola C, Moskowitz MA (1999) Pathobiology of ischaemic stroke: an integrated view. *Trends Neurosci* 22: 391–397.
- Fern R, Matute C (2019) Glutamate receptors and white matter stroke. *Neurosci Lett* 694: 86–92.
- Follett PL, Deng W, Dai W, Talos DM, Massillon LJ, Rosenberg PA, Volpe JJ, Jensen FE (2004) Glutamate receptor-mediated oligodendrocyte toxicity in periventricular leukomalacia: a protective role for topiramate. *J Neurosci* 24: 4412–4420.
- Ghasemlou N, Lopez-Vales R, Lachance C, Thuraingam T, Gaestel M, Radzich D, David S (2010) Mitogen-activated protein kinase-activated protein kinase 2 (mk2) contributes to secondary damage after spinal cord injury. *J Neurosci* 30: 13750–13759.
- Hara T, Abdulaziz-Umaru B, Sharifi K, Yoshikawa T, Owada Y, Kagawa Y (2020) Fatty acid binding protein 7 is involved in the proliferation of reactive astrocytes, but not in cell migration and polarity. *Acta Histochem Cytochem* 53: 73–81.
- Khwaja O, Volpe JJ (2008) Pathogenesis of cerebral white matter injury of prematurity. *Arch Dis Child Fetal Neonatal Ed* 93: F153–161.
- Kim EJ, Raval AP, Hirsch N, Perez-Pinzon MA (2010) Ischemic preconditioning mediates cyclooxygenase-2 expression via nuclear factor-kappa B activation in mixed cortical neuronal cultures. *Transl Stroke Res* 1: 40–47.
- Landi MT, Bertazzi PA, Shields PG, Clark G, Lucier GW, Garte SJ, Cosma G, Caporaso NE (1994) Association between CYP1A1 genotype, mRNA expression and enzymatic activity in humans. *Pharmacogenetics* 4: 242–246.
- Malta I, Moraes T, Rodrigues G, Franco P, Galdino G (2019) The role of oligodendrocytes in chronic pain: cellular and molecular mechanisms. *J Physiol Pharmacol* 70.
- Mangin JM, Li P, Scaffidi J, Gallo V (2012) Experience-dependent regulation of ng2 progenitors in the developing barrel cortex. *Nat Neurosci* 15: 1192–1194.
- Matute C (2010) Calcium dyshomeostasis in white matter pathology. *Cell Calcium* 47: 150–157.
- Matute C (2011) Glutamate and ATP signalling in white matter pathology. *J Anatomy* 219: 53–64.
- Merrill JE, Ignarro LJ, Sherman MP, Melinek J, Lane TE (1993) Microglial cell cytotoxicity of oligodendrocytes is mediated through nitric oxide. *J Immunol* 151: 2132–2141.
- Morin-Richaud C, Feldblum S, Privat A (1998) Astrocytes and oligodendrocytes reactions after a total section of the rat spinal cord. *Brain Res* 783: 85–101.
- Murugan M, Sivakumar V, Lu J, Ling EA, Kaur C (2011) Expression of N-methyl D-aspartate receptor subunits in amoeboid microglia mediates production of nitric oxide via NF-kB signaling pathway and oligodendrocyte cell death in hypoxic postnatal rats. *Glia* 59: 521–539.
- Nakajima K, Kohsaka S (1993) Functional roles of microglia in the brain. *Neurosci Res* 17: 187–203.

- Nowakowski RS, Lewin SB, Miller MW (1989) Bromodeoxyuridine immunohistochemical determination of the lengths of the cell cycle and the DNA-synthetic phase for an anatomically defined population. *J Neurocytol* 18: 311–318.
- Olivier P, Fontaine RH, Loron G, Van-Steenwinkel J, Biran V, Massonneau V, Kaindl A, Dalous J, Charriaut-Marlangue C, Aigrot MS, et al. (2009) Melatonin promotes oligodendroglial maturation of injured white matter in neonatal rats. *PLoS ONE* 4: e7128.
- Peferoen L, Kipp M, van der Valk P, van Noort JM, Amor S (2014) Oligodendrocyte-microglia cross-talk in the central nervous system. *Immunology* 14: 302–313.
- Peifer C, Wagner G, Laufer S (2006) New approaches to the treatment of inflammatory disorders small molecule inhibitors of p38 MAP kinase. *Curr Top Med Chem* 6: 113–149.
- Peixoto CA, de-Oliveira WH, Araújo SMD, Nunes AKS (2017) AMPK activation: Role in the signaling pathways of neuroinflammation and neurodegeneration. *Exp Neurol* 298: 31–41.
- Pekny M, Wilhelmsson U, Pekna M (2014) The dual role of astrocyte activation and reactive gliosis. *Neurosci Lett* 17: 30–38.
- Robinson MB, Lee ML, DaSilva S (2020) Glutamate transporters and mitochondria: signaling, co-compartmentalization, functional coupling, and future directions. *Neurochem Res* 45: 526–540.
- Saggu R, Schumacher T, Gerich F (2016) Astroglial NF- κ B contributes to white matter damage and cognitive impairment in a mouse model of vascular dementia. *Acta Neuropathol Commun* 4: 76.
- Saklatvala J (2004) The p38 MAP kinase pathway as a therapeutic target in inflammatory disease. *Curr Opin Pharmacol* 4: 372–377.
- Santa-Cecília FV, Socias B, Ouidja MO (2016) Doxycycline suppresses microglial activation by inhibiting the p38 MAPK and NF- κ B signaling pathways. *Neurotox Res* 29: 447–459.
- Sherwin C, Fern R (2005) Acute lipopolysaccharide-mediated injury in neonatal white matter glia: role of TNF- α , IL-1 β , and calcium. *J Immunol* 175: 155–161.
- Shimizu S, Narita M, Tsujimoto Y (1999) Bcl-2 family proteins regulate the release of apoptogenic cytochrome c by the mitochondrial channel VDAC. *Nature* 399 483–487.
- Sivakumar V, Ling EA, Lu J, Kaur C (2010) Role of glutamate and its receptors and insulin-like growth factors in hypoxia induced periventricular white matter injury. *Glia* 58: 507–523.
- Stoppini L, Buchs PA, Muller D (1991) A simple method for organotypic cultures of nervous tissue. *J Neurosci Methods* 37: 173–182.
- Volpe JJ (2009) Brain injury in premature infants: a complex amalgam of destructive and developmental disturbances. *Lancet Neurol* 8: 110–124.
- Wang L, Tu Y, Lin, Y (2016) CXCL5 signaling is a shared pathway of neuroinflammation and blood-brain barrier injury contributing to white matter injury in the immature brain. *J Neuroinflammation* 13: 6.
- Wu J, Yoo S, Wilcock D, Lytle JM, Leung PY, Colton CA, Wrathall JR (2010) Action of NG2(+) glial progenitors and microglia/macrophages from the injured spinal cord. *Glia* 58: 410–422.
- Xie QW, Kashiwabara Y, Nathan C (1994) Role of transcription factor NF- κ B/Rel in induction of nitric oxide synthase. *J Biol Chem* 269: 4705–4708.
- Yao SY, Ljunggren-Rose A, Chandramohan N, Whetsell Jr. WO, Sriram S (2010) In vitro and in vivo induction and activation of nNOS by LPS in oligodendrocytes. *J Neuroimmunol* 229: 146–156.
- Yi H, Bai Y, Zhu, X (2014) IL-17A induces MIP-1 α expression in primary astrocytes via Src/MAPK/PI3K/NF- κ B pathways: implications for multiple sclerosis. *J Neuroimmune Pharmacol* 9: 629–641.
- Yin G, Du M, Li R, Li K, Huang X, Duan D, Ai X, Yao F, Zhang L, Hu Z, et al. (2018) Glia maturation factor beta is required for reactive gliosis after traumatic brain injury in zebrafish. *Exp Neurol* 305: 129–138.